

# Phase-Aware Localization in Pinching Antenna Systems: CRLB Analysis and ML Estimation

Hao Feng, Ebrahim Bedeer, Ming Zeng, Xingwang Li, Shimin Gong, and Quoc-Viet Pham

**Abstract**—Pinching antenna systems (PASS) have recently emerged as a promising architecture for high-frequency wireless communications. In this letter, we investigate localization in PASS by jointly exploiting the received signal amplitude and phase information, unlike recent works that consider only the amplitude information. A complex baseband signal model is formulated to capture free-space path loss, waveguide attenuation, and distance-dependent phase rotation between the user and each pinching antenna. Using this model, we derive the Fisher information matrix (FIM) with respect to the user location and obtain closed-form expressions for the Cramér–Rao lower bound (CRLB) and the position error bound (PEB). A maximum likelihood (ML) estimator that jointly considers the received signal amplitude and phase is developed to estimate the unknown user location. Given the non-convexity of the estimation problem, a two-stage solution combining coarse grid search and Levenberg–Marquardt refinement is proposed. Numerical results demonstrate that the proposed phase-aware estimator outperforms existing amplitude-only method in terms of positioning accuracy.

**Index Terms**—Cramér–Rao lower bound (CRLB), pinching antenna systems (PASS), position error bound (PEB), maximum likelihood estimation, user localization.

## I. INTRODUCTION

Pinching antenna systems (PASS) have recently emerged as a promising architecture for high-frequency wireless communications, particularly in millimeter-wave (mmWave) and terahertz (THz) bands [1]–[4]. By enabling dynamically movable antenna ports along a dielectric waveguide, PASS provides a new degree of spatial flexibility that allows the system to effectively reconfigure its radiation and reception characteristics. This capability makes PASS especially attractive for restoring line-of-sight (LoS) connectivity, improving spectral efficiency, enhancing energy efficiency, and enabling adaptive beam control in challenging propagation environments [5]–[10].

Despite the rapid progress in PASS-related research, most existing works assume perfect knowledge of user locations and channel state information (CSI). Under these assumptions,

H. Feng is with Hunan Institute of Engineering, Xiangtan, China, and Donghua University, Shanghai, China as well as Laval University, Quebec city, Canada (email: 1219001@mail.dhu.edu.cn).

E. Bedeer is with University of Saskatchewan, Saskatoon, SK, Canada (email: e.bedeer@usask.ca).

M. Zeng is with Laval University, Quebec City, Canada (email: ming.zeng@ge1.ulaval.ca).

X. Li is with Henan Polytechnic University, Jiaozuo, China (email: lixingwang@hpu.edu.cn).

S. Gong is with Sun Yat-sen University, Guangzhou, China (e-mail: gongsh5@mail.sysu.edu.cn).

Q.-V. Pham is School of Computer Science and Statistics, Trinity College Dublin, Dublin 2, D02PN40, Ireland (e-mail: Viet.Pham@tcd.ie).

various resource allocation, beamforming, and power optimization strategies have been developed. However, in practical communication systems, accurate CSI acquisition is costly and user positions are generally unknown or imperfectly estimated. The performance of PASS is fundamentally geometry-dependent due to the waveguide attenuation and distance-sensitive phase rotation. Consequently, inaccurate user positioning directly degrades both communication reliability and resource allocation efficiency.

Recent efforts have relaxed these idealized assumptions. Channel estimation techniques for PASS have been investigated in [11], [12], and robust resource allocation schemes under user location uncertainty have been proposed in [13]–[15]. Moreover, user positioning in PASS has been preliminarily studied in [16], where localization relies solely on the received signal amplitude information. However, neglecting phase information discards a substantial portion of the useful information embedded in the received signals. In LoS-based systems, phase variations are highly sensitive to propagation distance, suggesting that amplitude-only approaches are intrinsically suboptimal from an estimation-theoretic standpoint.

Motivated by these observations, this work develops a comprehensive framework for user localization in PASS that jointly exploits both received signal amplitude and phase. Unlike prior amplitude-only schemes, the proposed formulation leverages the full complex baseband signal model, thereby fully capturing the geometric and wave propagation characteristics of PASS. The main contributions of this paper are summarized as follows:

- **Unified Signal Model for Localization in PASS:** We establish a rigorous signal model that incorporates free-space path loss, waveguide attenuation, and phase rotation. This model explicitly reveals how user position affects both amplitude and phase of the received signal across sequentially activated pinching antennas.
- **Closed-form Characterization of Localization Accuracy:** We derive the Fisher information matrix (FIM) and obtain closed-form expressions for the Cramér–Rao lower bound (CRLB) and the position error bound (PEB); characterizing the fundamental limits of localization accuracy. The resulting expressions clearly separate geometric sensitivity and distance-dependent amplitude–phase sensitivity, providing valuable insight into how the system parameters, e.g., antenna placement and waveguide parameters, influence localization accuracy.
- **Two-Stage Maximum Likelihood Localization Algorithm:** We develop a maximum likelihood (ML) estimator that jointly considers the received signal amplitude

and phase to estimate the unknown user location. Given the non-convexity of the likelihood function, a two-stage solution combining coarse grid search and Levenberg–Marquardt refinement is further proposed. Numerical results show that the proposed phase-aware ML estimator significantly outperforms the weighted least squares estimator developed in [16], which relies only on the amplitude information, in terms of positioning accuracy.

## II. SYSTEM MODEL

We consider an uplink communication scenario in which  $K$  single-antenna users communicate with an access point (AP) through  $N$  pinching antennas (PAs) deployed on a single dielectric waveguide. The  $K$  users are uniformly distributed on the ground plane within a rectangular area of dimension  $\ell_1 \times \ell_2$  meters. The system operates using time division multiplexing, where only one user transmits in a given time slot. The AP will activate the  $N$  PAs one by one to receive the signal from the  $k$ th user to help with the localization as explained later in this section. The sequential PA scan is assumed fast enough such that the user location remains fixed and the noise samples are independent.

We assume the feed point is located at  $\mathbf{v}_0 = [0, 0, d]^\top$ , and the dielectric waveguide, of length  $\ell_w \leq \ell_2$ , is located along the  $y$ -axis at height  $d$  above the ground plane. Hence, the location of the  $n$ th PA,  $n = 1, \dots, N$ , is denoted as  $\mathbf{v}_n = [0, v_n, d]^\top$  where  $v_n \in [0, \ell_w]$ . The  $K$  users are located on the ground floor, i.e.,  $z = 0$ . Hence, the 2D location of the  $k$ th user,  $k = 1, \dots, K$ , is  $\mathbf{u}_k = [u_{x,k}, u_{y,k}]^\top$ . We assume that the user location  $\mathbf{u}_k$  is unknown and needs to be estimated.

The combined channel  $h_{k,n}$  from user  $k$  to the AP consists of 1) the large-scale channel, 2) the small-scale fading, and 3) the attenuation inside the dielectric waveguide. The large-scale channel is mainly due to free-space loss and under LoS assumption it is given by [5]

$$h_{k,n}^{(\text{ls})}(d_{k,n}) = \frac{\lambda}{4\pi d_{k,n}}, \quad (1)$$

where  $\lambda$  is the wavelength and  $d_{k,n}$  is the distance from the  $k$ th user to the  $n$ th PA, which is given by

$$d_{k,n} = \sqrt{u_{x,k}^2 + (u_{y,k} - v_n)^2 + d^2}. \quad (2)$$

The small scale fading is modeled as

$$h_{k,n}^{(\text{ss})}(d_{k,n}) = \gamma_{k,n} e^{-j2\pi d_{k,n}/\lambda}, \quad (3)$$

where  $\gamma_{k,n}$  is the channel gain. The attenuation inside the dielectric waveguide is modeled as [17]

$$h_n^{(\text{w})} = e^{-(\alpha+j\beta)v_n}, \quad (4)$$

where  $\alpha = \pi\sqrt{\epsilon_r} \tan(\delta)/\lambda$  and  $\beta = 2\pi\sqrt{\epsilon_r}/\lambda$ , with  $\epsilon_r$  and  $\tan(\delta)$  representing the relative permittivity and loss angle tangent, respectively [17].

The received signal at the AP coming from the  $k$ th user through the  $n$ th PA is given by

$$\begin{aligned} r_{k,n} &= h_{k,n}^{(\text{ls})}(d_{k,n}) h_{k,n}^{(\text{ss})}(d_{k,n}) h_n^{(\text{w})} \sqrt{p_k} s_k + w_{k,n} \\ &= \frac{\gamma_{k,n} a_{k,n}}{d_{k,n}} e^{-j2\pi d_{k,n}/\lambda} s_k + w_{k,n}, \quad \forall k, \end{aligned} \quad (5)$$

where  $a_{k,n} = \lambda\sqrt{p_k} e^{-(\alpha+j\beta)v_n}/4\pi$ ,  $p_k$  and  $s_k$  are the transmit power and the unit-power transmit pilot symbol, respectively, and  $w_{k,n}$  is the zero-mean additive white Gaussian noise (AWGN) with variance  $\sigma^2$ . Following [16], we assume that the channel gain is normalized, i.e.,  $\gamma_{k,n} = 1$ .

Given that the noise samples  $w_{k,n}$ ,  $n = 1, \dots, N$ , are independent and identically distributed, the joint probability density function (PDF) of all received signals from all  $N$  PAs for the user  $k$  can be expressed as

$$f_{\mathbf{u}_k}(\mathbf{r}_k | \mathbf{u}_k) = \frac{1}{(\pi\sigma^2)^N} \exp\left(-\frac{\|\mathbf{r}_k - \mathbf{s}_k(\mathbf{u}_k)\|^2}{\sigma^2}\right), \quad (6)$$

where  $\mathbf{r}_k = [r_{k,1}, \dots, r_{k,N}]^\top$  and  $\mathbf{s}_k(\mathbf{u}_k) = [(\gamma_{k,1} a_{k,1}/d_{k,1}) e^{-j2\pi d_{k,1}/\lambda} s_k, \dots, (\gamma_{k,N} a_{k,N}/d_{k,N}) e^{-j2\pi d_{k,N}/\lambda} s_k]^\top$ . Hence, the log-likelihood function  $L_{\mathbf{r}_k}(\mathbf{u}_k)$  is given as

$$L_{\mathbf{r}_k}(\mathbf{u}_k) \propto -\frac{1}{\sigma^2} (\mathbf{r}_k - \mathbf{s}_k(\mathbf{u}_k))^H (\mathbf{r}_k - \mathbf{s}_k(\mathbf{u}_k)), \quad (7)$$

where  $(\cdot)^H$  denotes the conjugate transpose operation.

## III. CRLB DERIVATION AND ANALYSIS

The FIM can be written as

$$\mathbf{J}(\mathbf{u}_k) = \frac{2}{\sigma^2} \Re \left\{ \left( \frac{\partial \mathbf{s}_k(\mathbf{u}_k)}{\partial \mathbf{u}_k} \right)^H \frac{\partial \mathbf{s}_k(\mathbf{u}_k)}{\partial \mathbf{u}_k} \right\}, \quad (8)$$

where  $\frac{\partial \mathbf{s}_k(\mathbf{u}_k)}{\partial \mathbf{u}_k} \in \mathbb{C}^{N \times 2}$  is the Jacobian matrix of the signal vector  $\mathbf{s}_k(\mathbf{u}_k)$  with respect to the  $k$ th user location  $\mathbf{u}_k$ . With the help of the chain rule, one can show that

$$\begin{aligned} \frac{\partial s_{k,n}}{\partial u_{x,k}} &= \frac{\partial s_{k,n}}{\partial d_{k,n}} \frac{\partial d_{k,n}}{\partial u_{x,k}}, \\ &= a_{k,n} s_k e^{-j\frac{2\pi}{\lambda} d_{k,n}} \left( -\frac{u_{x,k}}{d_{k,n}^3} - j\frac{2\pi}{\lambda} \frac{u_{x,k}}{d_{k,n}^2} \right), \end{aligned} \quad (9)$$

Similarly, one can calculate

$$\frac{\partial s_{k,n}}{\partial u_{y,k}} = a_{k,n} s_k e^{-j\frac{2\pi}{\lambda} d_{k,n}} \left( -\frac{u_{y,k} - v_n}{d_{k,n}^3} - j\frac{2\pi}{\lambda} \frac{u_{y,k} - v_n}{d_{k,n}^2} \right). \quad (10)$$

One can re-write (9) and (10), respectively, as

$$\frac{\partial s_{k,n}}{\partial u_{x,k}} = -m_{k,n}(d_{k,n}) u_{x,k}, \quad (11)$$

$$\frac{\partial s_{k,n}}{\partial u_{y,k}} = -m_{k,n}(d_{k,n}) (u_{y,k} - v_n), \quad (12)$$

where  $m_{k,n}(d_{k,n}) = a_{k,n} s_k e^{-j\frac{2\pi}{\lambda} d_{k,n}} \left( \frac{1}{d_{k,n}^3} + j\frac{2\pi}{\lambda} \frac{1}{d_{k,n}^2} \right)$ . Hence,

$$\frac{\partial \mathbf{s}_k(\mathbf{u}_k)}{\partial \mathbf{u}_k} = -m_{k,n}(d_{k,n}) [u_{x,k}, (u_{y,k} - v_n)], \quad (13)$$

and

$$\frac{\partial \mathbf{s}_k(\mathbf{u}_k)}{\partial \mathbf{u}_k} = -\mathbf{M}_k(d_{k,n}) \mathbf{G}(\mathbf{u}_k), \quad (14)$$

where  $\mathbf{G}(\mathbf{u}_k) = [\mathbf{g}_1^\top; \dots; \mathbf{g}_N^\top] \in \mathbb{R}^{N \times 2}$ ,  $\mathbf{g}_n^\top = [u_{x,k}, (u_{y,k} - v_n)]$ , and  $\mathbf{M}_k(d_{k,n}) = \text{diag}(m_{k,1}(d_{k,1}), \dots, m_{k,N}(d_{k,N})) \in \mathbb{C}^{N \times N}$ , with  $\text{diag}(\cdot)$  denoting the diagonal matrix. Please note

that  $\mathbf{M}(d_{k,n})$  captures the amplitude and phase sensitivities with respect to distance  $d_{k,n}$ , while  $\mathbf{G}(\mathbf{u}_k)$  captures the geometric sensitivity of the distance with respect to the user location  $\mathbf{u}_k$ . Hence, the FIM can be reformulated as

$$\mathbf{J}(\mathbf{u}_k) = \frac{2}{\sigma^2} \Re \left\{ \mathbf{G}(\mathbf{u}_k)^H \tilde{\mathbf{M}}_k(d_{k,n}) \mathbf{G}(\mathbf{u}_k) \right\}, \quad (15)$$

where  $\tilde{\mathbf{M}}_k(d_{k,n}) = \mathbf{M}_k(d_{k,n})^H \mathbf{M}_k(d_{k,n}) = \text{diag}(|m_{k,1}(d_{k,1})|^2, \dots, |m_{k,N}(d_{k,N})|^2) \in \mathbb{R}^{N \times N}$ . Please note that  $\tilde{\mathbf{M}}_k(d_{k,n})$  captures only the magnitude-squared sensitivity with respect to the distance  $d_{k,n}$ .

The CRLB for the unbiased estimator  $\hat{\mathbf{u}}_k$  is given as

$$\begin{aligned} \text{Cov}(\hat{\mathbf{u}}_k) &\succeq \mathbf{J}^{-1}(\mathbf{u}_k) \\ &\succeq \frac{1}{J_{11}J_{22} - J_{12}^2} \begin{bmatrix} J_{22} & -J_{12} \\ -J_{21} & J_{11} \end{bmatrix}, \end{aligned} \quad (16)$$

where  $J_{11}$ ,  $J_{12}$ ,  $J_{21}$ , and  $J_{22}$  are the block matrices of the FIM  $\mathbf{J}(\mathbf{u}_k)$  whose elements are given as

$$J_{11} = \frac{2}{\sigma^2} \sum_{n=1}^N |m_{k,n}(d_{k,n})|^2 u_{x,k}^2, \quad (17)$$

$$J_{12} = J_{21} = \frac{2}{\sigma^2} \sum_{n=1}^N |m_{k,n}(d_{k,n})|^2 u_{x,k}(u_{y,k} - v_n), \quad (18)$$

$$J_{22} = \frac{2}{\sigma^2} \sum_{n=1}^N |m_{k,n}(d_{k,n})|^2 (u_{y,k} - v_n)^2. \quad (19)$$

Then, the lower bound of the variance of the estimates  $\hat{u}_{x,k}$  and  $\hat{u}_{y,k}$  are given as

$$\text{Var}(\hat{u}_{x,k}) \geq [\text{Cov}(\hat{\mathbf{u}}_k)]_{11} = \frac{J_{22}}{J_{11}J_{22} - J_{12}^2}, \quad (20)$$

$$\text{Var}(\hat{u}_{y,k}) \geq [\text{Cov}(\hat{\mathbf{u}}_k)]_{22} = \frac{J_{11}}{J_{11}J_{22} - J_{12}^2}. \quad (21)$$

Finally, the PEB is expressed as

$$\text{PEB}_k = \sqrt{\text{Tr}\{\text{Cov}(\hat{\mathbf{u}}_k)\}} = \left( \frac{J_{11} + J_{22}}{J_{11}J_{22} - J_{12}^2} \right)^{\frac{1}{2}}, \quad (22)$$

where  $\text{Tr}\{\cdot\}$  denotes the trace operation.

#### IV. MAXIMUM LIKELIHOOD ESTIMATION OF THE USER LOCATION

As one can see from (7), the likelihood function  $L_{\mathbf{r}_k}(\mathbf{u}_k)$  is non-convex in the user location  $\mathbf{u}_k$ , as  $\mathbf{u}_k$  appears in non-linear terms in the denominator and the exponent of  $s_k(\mathbf{u}_k)$ . To address it, we employ the following two-steps algorithm to find the user location.

First, we discretize the ground plane into a grid spaced by  $d_{\text{grid}} = \lambda/4$  to obtain initial user locations  $\mathbf{u}_{k,\text{initial}}$ . For each initial point  $\mathbf{u}_{k,\text{initial}}$ , we calculate the residual error as

$$\tilde{f}_{\text{error}}(\mathbf{u}_{k,\text{initial}}) = (\mathbf{r}_k - \mathbf{s}_k(\mathbf{u}_{k,\text{initial}}))^H (\mathbf{r}_k - \mathbf{s}_k(\mathbf{u}_{k,\text{initial}})). \quad (23)$$

Then, we identify the smallest  $N_u$  values of  $\tilde{f}_{\text{error}}(\mathbf{u}_{k,\text{initial}})$  such that each one of them will be an input to the second step. This coarse grid search helps identify promising initial points and mitigate the risk of convergence to poor local minima.

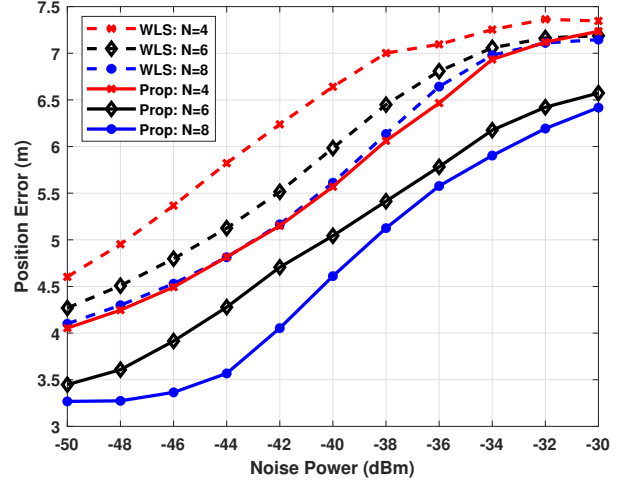


Fig. 1: Position error versus noise power under different number of PAs.

In the second step, we adopt the Levenberg-Marquardt (LM) algorithm [18] for each of the  $N_u$  values to refine the estimates of the user location  $\hat{\mathbf{u}}_k$  in iterative manner. In particular, for iteration  $i$ , the updated user location is calculated as

$$\hat{\mathbf{u}}_k^{(i+1)} = \hat{\mathbf{u}}_k^{(i)} + \Delta \hat{\mathbf{u}}_k^{(i)}, \quad (24)$$

where the update step  $\Delta \hat{\mathbf{u}}_k^{(i)}$  at iteration  $i$  is calculated by solving the following linear system

$$\begin{aligned} &\left( \frac{\partial \mathbf{s}_k^H(\hat{\mathbf{u}}_k^{(i)})}{\partial \hat{\mathbf{u}}_k^{(i)}} \frac{\partial \mathbf{s}_k(\hat{\mathbf{u}}_k^{(i)})}{\partial \hat{\mathbf{u}}_k^{(i)}} + \lambda_{\text{LM}} \mathbf{I} \right) \Delta \hat{\mathbf{u}}_k^{(i)} \\ &= \Re \left\{ \frac{\partial \mathbf{s}_k^H(\hat{\mathbf{u}}_k^{(i)})}{\partial \hat{\mathbf{u}}_k^{(i)}} \left[ \mathbf{r}_k - \mathbf{s}_k(\hat{\mathbf{u}}_k^{(i)}) \right] \right\}, \end{aligned} \quad (25)$$

where  $\frac{\partial \mathbf{s}_k(\hat{\mathbf{u}}_k^{(i)})}{\partial \hat{\mathbf{u}}_k^{(i)}}$  is the Jacobian matrix calculated as in (14) and  $\lambda_{\text{LM}}$  is the damping factor.

In the end, we select the final user location among the  $N_u$  updated locations that minimize the likelihood function in (7).

#### V. NUMERICAL RESULTS

Numerical results are presented in this section to evaluate the performance of the proposed phase-aware user position estimation method and to compare it with the weighted least squares (WLS) approach reported in [16]. For a fair comparison, we adopt the same simulation setup and system parameters as in [16]. Specifically, the considered deployment area is a rectangular region of size  $6 \times 10 \text{ m}^2$ , and the waveguide height is set to  $d = 3 \text{ m}$ . The subcarrier frequency is 2.8 GHz, and the user transmit power is fixed at  $p_k = 0.1 \text{ W}$ . The relative permittivity and dielectric loss tangent are  $\epsilon_r = 2.08$  and  $\tan(\delta) = 0.0004$ , respectively, following [17]. The number of initially identified user location  $N_u$  is 20. Unless otherwise specified, all results are averaged over 1000 independent random realizations to ensure statistical reliability.

Figure 1 illustrates the position estimation error as a function of the noise power for different numbers of PAs. In the

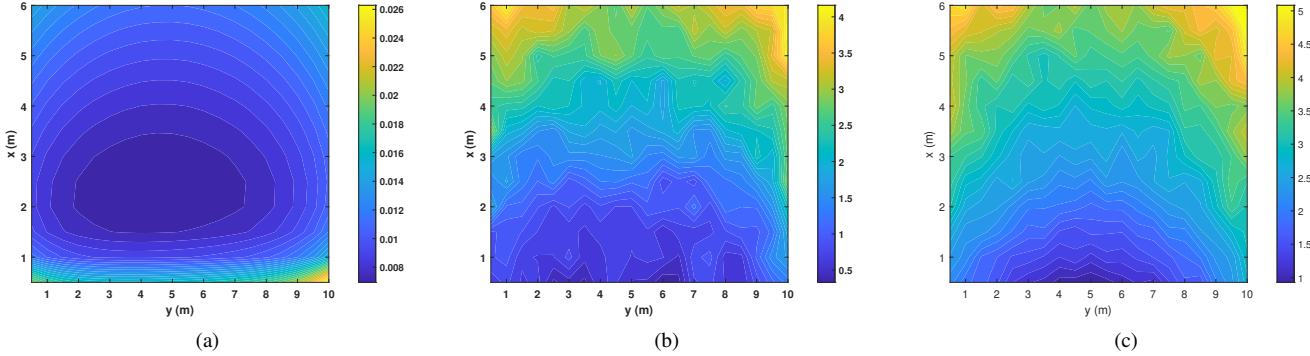


Fig. 2: Position error map (m) for: a) PEB; b) Proposed solution and c) Benchmark from [16]. Here  $N = 8$  and the noise power is  $-40$  dBm. Each point is obtained by averaging over 100 random trials for b) and c).

figure, “WLS” denotes the benchmark method from [16] that relies only on the amplitude information, whereas “Prop” represents the proposed algorithm that considers both amplitude and phase information. As one can see, for both schemes, the localization error increases monotonically with the noise power due to the degradation of the received SNR. Increasing the number of PAs improves the spatial diversity and geometric resolution, thereby reducing the position error. Importantly, for any given number of PAs, the proposed method consistently achieves lower estimation error than the WLS benchmark, demonstrating its clear performance advantage.

Figure 2 further compares the spatial distribution of the position error obtained from: the theoretical PEB, the proposed method, and the WLS benchmark in [16]. The error maps of the proposed and benchmark schemes exhibit similar spatial patterns, where larger errors occur when the user is located farther from the PAs. This behavior is primarily attributed to reduced received SNR and weaker geometric diversity at larger distances. Nevertheless, across the entire coverage area, the proposed method yields uniformly lower estimation errors than the benchmark. In contrast, the theoretical PEB remains significantly lower than the practical estimation errors of both schemes, indicating the existence of a non-negligible performance gap and suggesting potential room for further algorithmic optimization.

## VI. CONCLUSION

This letter investigated user localization in pinching antenna systems by fully exploiting the complex baseband signal structure. Unlike prior amplitude-only approaches, the proposed framework jointly utilizes amplitude and phase information, thereby capturing the intrinsic distance-sensitive characteristics of PASS. Closed-form CRLB and PEB expressions were derived, providing theoretical insight into how the system parameters, e.g., antenna placement and waveguide parameters, affect positioning accuracy. A practical two-stage maximum likelihood estimator was developed to address the non-convex localization problem. Numerical results verified that the proposed method consistently outperforms the existing weighted least squares benchmark and significantly reduces positioning error across different noise levels and antenna configurations.

## REFERENCES

- [1] A. Fukuda *et al.*, “Pinching antenna using a dielectric waveguide as an antenna,” *Technical Journal*, vol. 23, no. 3, pp. 5–12, Jan. 2022.
- [2] M. Zeng, J. Wang, O. A. Dobre, Z. Ding, G. K. Karagiannidis, R. Schober, and H. V. Poor, “Resource allocation for pinching-antenna systems: State-of-the-art, key techniques and open issues,” 2025. [Online]. Available: <https://arxiv.org/abs/2506.06156>
- [3] Y. Liu, Z. Wang, X. Mu, C. Ouyang, X. Xu, and Z. Ding, “Pinching-antenna systems: Architecture designs, opportunities, and outlook,” *IEEE Commun. Mag.*, pp. 1–7, Jan. 2025.
- [4] Z. Yang *et al.*, “Pinching antennas: Principles, applications and challenges,” *IEEE Wirel. Commun.*, pp. 1–10, Oct. 2025.
- [5] Z. Ding, R. Schober, and H. Vincent Poor, “Flexible-antenna systems: A pinching-antenna perspective,” *IEEE Trans. Commun.*, vol. 73, no. 10, pp. 9236–9253, Oct. 2025.
- [6] M. Zeng, J. Wang, X. Li, G. Wang, O. A. Dobre, and Z. Ding, “Sum rate maximization for NOMA-assisted uplink pinching-antenna systems,” *IEEE Wirel. Commun. Lett.*, vol. 15, pp. 280–284, 2026.
- [7] J. Zhao *et al.*, “Pinching-antenna systems-enabled multi-user communications: Transmission structures and beamforming optimization,” *IEEE Trans. Commun.*, pp. 1–1, Dec. 2025.
- [8] M. Zeng, X. Li, J. Wang, G. Huang, O. A. Dobre, and Z. Ding, “Energy-efficient resource allocation for NOMA-assisted uplink pinching-antenna systems,” *IEEE Wirel. Commun. Lett.*, vol. 14, no. 11, pp. 3695–3699, Nov. 2025.
- [9] Y. Fu, F. He, Z. Shi, and H. Zhang, “Power minimization for noma-assisted pinching antenna systems with multiple waveguides,” 2025. [Online]. Available: <https://arxiv.org/abs/2503.20336>
- [10] S. A. Tegos, P. D. Diamantoulakis, Z. Ding, and G. K. Karagiannidis, “Minimum data rate maximization for uplink pinching-antenna systems,” *IEEE Wirel. Commun. Lett.*, vol. 14, no. 5, pp. 1516–1520, May 2025.
- [11] J. Xiao, J. Wang, and Y. Liu, “Channel estimation for pinching-antenna systems (PASS),” *IEEE Commun. Lett.*, vol. 29, no. 8, pp. 1789–1793, Aug. 2025.
- [12] G. Zhou, V. K. Papanikolaou, Z. Ding, and R. Schober, “Channel estimation for mmwave pinching-antenna systems,” in *Proc. IEEE SPAWC*, Jul. 2025, pp. 1–5.
- [13] M. Zeng, X. Wang, Y. Liu, Z. Ding, G. K. Karagiannidis, and H. V. Poor, “Robust resource allocation for pinching-antenna systems under user location uncertainty,” *IEEE Trans. Veh. Tech.*, pp. 1–5, 2026.
- [14] H. Feng, M. Zeng, X. Li, W. Xie, N. Xia, and O. A. Dobre, “Joint power allocation and antenna placement for pinching-antenna systems under user location uncertainty,” 2026. [Online]. Available: <https://arxiv.org/abs/2601.19704>
- [15] M. Sun, C. Ouyang, S. Wu, and Y. Liu, “Robust beamforming for pinching-antenna systems,” *IEEE Trans. Veh. Tech.*, pp. 1–6, 2026.
- [16] Y. Zhang, X. Sun, J. Wang, T. Hou, A. Li, Y. Liu, and A. Nallanathan, “Pinching-antenna systems (PASS)-based indoor positioning,” 2025. [Online]. Available: <https://arxiv.org/abs/2508.08185>
- [17] R. S. Rao, *Microwave engineering*. PHI Learning Pvt. Ltd., 2015.
- [18] K. Levenberg, “A method for the solution of certain non-linear problems in least squares,” *Quarterly of Applied Mathematics*, vol. 2, no. 2, pp. 164–168, 1944.